

STEEL DENSITY CHANGE UNDER SUPERDEEP-PENETRATION CONDITIONS

S. K. Andilevko, E. A. Doroshkevich,
S. S. Karpenko, S. M. Usherenko, and
V. A. Shilkin

UDC 534.2

A series of target density measurements under superdeep-penetration conditions is made. The influence of different factors accompanying this process on target density change is evaluated experimentally.

Introduction. In research studies devoted to investigation of the superdeep-penetration effect [1-3] a considerable change in the structure of the target material, in particular, steel, has been noticed near the trajectory of particle motion. Here, intense plastic strain of the target material was recorded in a zone of $1-2d$ in the immediate vicinity of the collapsed channel formed by the particle in penetration into the target. Often the center of this zone with a diameter of about $0.3d$ (Fig. 1) is filled with target material whose structure has practically lost its crystalline ordering, as evidenced by the x-ray photograph given in Fig. 2a for the channel segment depicted in Fig. 2b. Microanalyzer-aided investigations [4, 5] have revealed the presence of the introduced powder material in considerable amounts (up to 10-12% of the mass) in the segments under observation, which points to a change in physicochemical parameters of the target substance in these zones. Around detected fragments of powder particles (Figs. 3, 4), zones with a considerable amount of introduced material contained in them whose dimensions correspond approximately to the dimensions of the penetrating particles are also formed. Therefore it is assumed that the change in physicochemical properties of the target material due to realization of the superdeep-penetration (SDP) effect can be detected by simple methods and allows the concentration of the introduced material to be judged by the absolute magnitude of this change.

As the first step in an investigation of the dependence of the physicochemical properties of a target on the amount of introduced material, we carried out a series of experiments on density measurement of a steel target after its treatment by the SDP procedure with tungsten, iron, and Al_2O_3 powders under the same conditions of its loading in accordance with the scheme given in [1].

1. Experimental Procedure. After treatment with a flux of powder particles a cylindrical steel sample with an initial density $\rho_0 = 7.8579 \text{ g/cm}^3$ was cut along the symmetry axis in the direction of flow input. The halves obtained were divided along the cutting plane into specimens with a mass of about 3 g (see the scheme in Fig. 5). To determine the substance density, we used the procedure of weighing the specimens in two media (air and distilled water). To avoid large errors in weighing in the liquid, all the surfaces of the specimens were polished, which allowed us to prevent accumulation of large air bubbles near surface microirregularities. Each specimen was weighed twice on an analytical balance with an accuracy of up to 0.0001 g. Here, its mass was determined in air (P_a) and in water (P_w). The density of the weighed specimen ρ was calculated by the formula

$$\rho = \frac{\rho_w (P_a - P_{th}) - \rho_a (P_w - P_{th})}{P_a - P_w} \quad (1)$$

2. Experiment. The change in the density of a target as a result of loading the latter by a high-speed dense flux of powder particles with parameters typical for SDP [1-4] can be attributed to several simultaneously occurring processes:

Research Institute of Pulsed Processes of the Belarusian Republican Powder Metallurgy Association, Minsk. Translated from *Inzhenerno-Fizicheskii Zhurnal*, Vol. 71, No. 3, pp. 394-398, May-June, 1998. Original article submitted April 12, 1996.

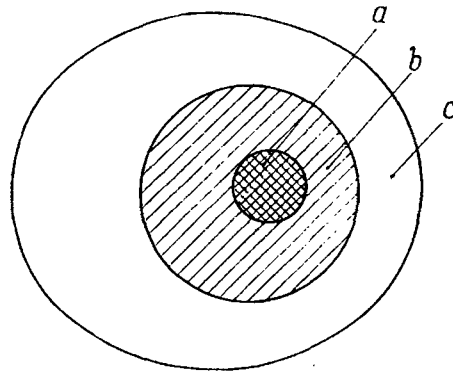


Fig. 1. Structure of the channel zone recorded in the target after the SDP effect: a) central region filled practically by a destructurized mixture of the target material and the particles; b) region of intense plastic deformation; c) region of weak plastic deformation.

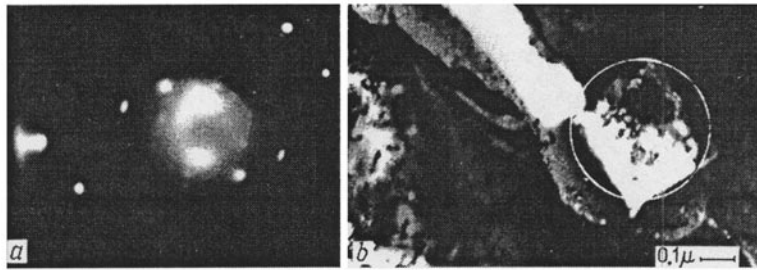


Fig. 2. Cross section of the channel formed by a particle after etching of the central region: a) x-ray photograph; b) view under a transmission electron microscope.

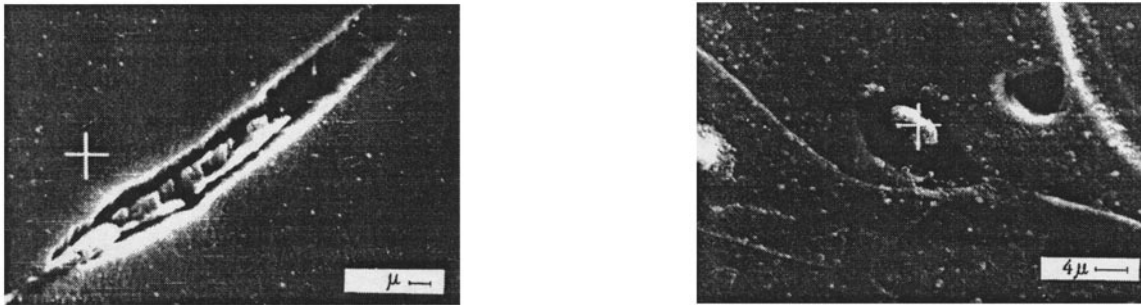


Fig. 3. Fibers formed near the axis of penetrating-particle motion.

Fig. 4. Remaining part of a TiB_2 particle in the target at a depth of about 6 mm.

- a) introduction of a material of different density into the target;
- b) intense plastic deformation of the target material in the zones of particle penetration;
- c) plastic deformation of the target surface in its interaction with the powder-particle flux (strain hardening);
- d) crystallochemical interaction of the particle and target materials in the channel zone at the considerable pressures and temperatures realized there (up to 30 GPa and 3000 K, respectively);
- e) loosening of the target material due to introduction of gas components entrained by the flux of powder particles in the course of its formation.

In this stage, our task was to evaluate the influence of the factors enumerated above on the change in the target density under superdeep-penetration conditions. To reach this goal, we chose a number of powders for

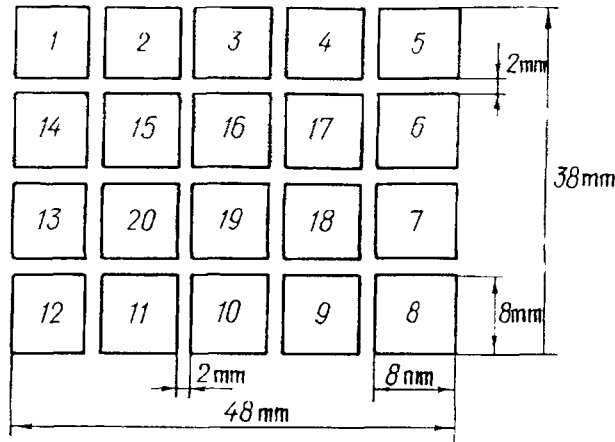


Fig. 5. Scheme of cutting the target into specimens. The figures are the numbers of the specimens.

TABLE 1. Density Measurement Results for Steel Specimens after Their Treatment with Various Powders

Specimen No.	ρ/ρ_0			
	W	Fe, $d < 50 \mu\text{m}$	Fe, $d \geq 315 \mu\text{m}$	Al_2O_3
1	1.000000	0.999952	1.000901	1.000637
2	1.005943	1.000056	0.999780	0.999327
3	1.006253	1.000580	0.999646	0.997947
4	1.006819	0.999700	0.999875	1.000325
5	—	1.000310	1.000544	0.999472
6	—	1.000284	1.000247	1.000912
7	—	1.999537	1.000854	0.999280
8	—	1.000869	1.000374	0.999518
9	1.010658	1.000644	0.999971	0.999864
10	1.008111	1.000979	1.001014	0.999443
11	1.007797	1.001587	0.999823	0.999091
12	1.009417	1.001046	0.999989	0.999214
13	1.009033	—	1.000264	1.000083
14	1.008692	1.000154	1.001740	0.998904
15	1.006602	1.000344	1.001012	0.999623
16	1.008968	1.000601	1.001622	1.000383
17	1.008704	1.000839	0.999513	0.999120
18	1.009222	0.999917	0.999837	—
19	1.009681	1.000073	0.999830	0.999409
20	1.010589	1.001184	0.999417	0.998455

formation of a high-speed dense flux: iron with a particle size $< 50 \mu\text{m}$ and $> 315 \mu\text{m}$; W and Al_2O_3 with a particle size $< 50 \mu\text{m}$.

Target treatment by a flux of iron powder particles with $d > 315 \mu\text{m}$ allowed evaluation of the influence of factor c) on the density change of the target since in the present scheme the SDP effect is realized only for particles with an initial size $d < 100 \mu\text{m}$ [1-5]. Here, it should be taken into account that a near-surface target

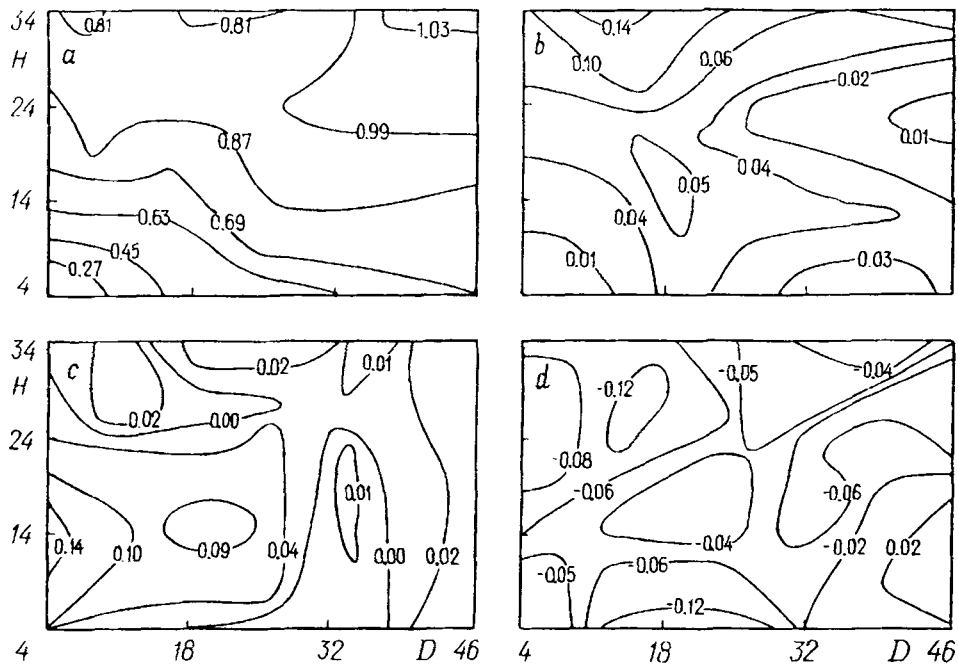


Fig. 6. Density change of steel under its treatment with powders of tungsten (a), iron (b: $d > 315 \mu\text{m}$, c: $d < 50 \mu\text{m}$), and aluminum oxide (d) in percent of ρ_0 . The treatment is performed from bottom to top. D, H , mm.

layer with a thickness of 2–3 mm was removed to preclude the influence of the macrocrater on the measurement results.

Introduction of iron powder particles with $d < 50 \mu\text{m}$ into the target is accompanied by formation of a channel structure and can be used as a basis for evaluation of the influence of factor b) on the density change of the target. The influence of factor a) manifests itself upon changing the flux density, i.e., in using W and Al_2O_3 powders for loading purposes. Factor d) must be manifested in iron treatment by tungsten powder since Al_2O_3 practically does not interact with iron. The most difficult task is to take into account the influence of factor e); however it can be considered to be approximately the same for all powders with $d < 50 \mu\text{m}$ used in the experiment, and therefore in determination of the comparative characteristics of the density change this factor has not been taken into consideration.

3. Experimental Results. Calculated densities for different specimens are given in Table 1. Figure 6a presents results of statistical processing of data on the density change of steel subjected to treatment by the tungsten powder in percent of the initial value $\rho_0 = 7.8579 \text{ g/cm}^3$. In the same procedure, data are given on treatment of a steel specimen by iron powder with a particle greater size than $315 \mu\text{m}$ (Fig. 6b) and less than $50 \mu\text{m}$ (Fig. 6c) as well as by the Al_2O_3 powder (Fig. 6d).

The mean value of the density throughout the target can be calculated as some integral characteristic of the contribution of all three components. For the tungsten-steel pair it amounted to 0.843%, for the iron ($d < 50 \mu\text{m}$)-steel pair 0.044%, for the iron ($d > 315 \mu\text{m}$)-steel pair 0.030%, and for the Al_2O_3 -steel pair 0.046%. Thus, the mean density change as a whole in a specimen due to introduction of the tungsten powder is approximately 0.799%, and for Al_2O_3 0.090%.

Figure 7 presents isolines of the density change of the target in percent of the initial value $\rho_0 = 7.8579 \text{ g/cm}^3$ as a function of the density of the introduced material and the target depth (a) and of the density of the introduced material and the diameter of the treated target (b). Both dependences can be used as calibration curves for determination of the density and concentration of the introduced particles. For this, the following formula should be used:

$$C = |q| \frac{\rho_0}{\rho_p}, \quad (2)$$

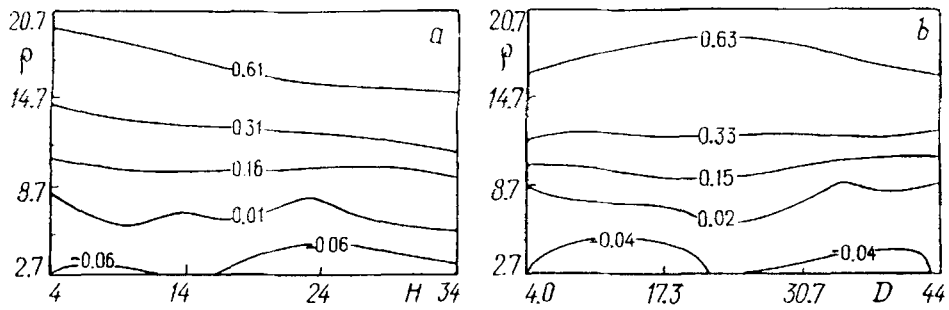


Fig. 7. Density change of a steel specimen as a function of the density of the introduced powder and the depth (a) and diameter (b) of the target. ρ , g/cm³.

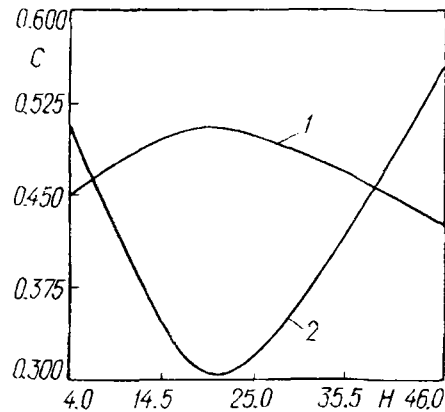


Fig. 8. Curves of the concentration change of W and Al₂O₃ as a function of the target depth (averaged values): 1) steel treated with Al₂O₃; 2) the same, W. C, %.

where

$$q = q_{\text{meas}} - q_{\text{Fe50}}, \quad (3)$$

is the resultant deviation due to factors b), c), and e). In particular, the averaged concentration over the entire target is 0.32% (of the mass) for W and 0.28% for Al₂O₃. The concentration change for W and Al₂O₃ versus the target depth is shown in Fig. 8.

Conclusions. The experiments described in the present work have allowed us to evaluate the density change in steel as a consequence of the superdeep-penetration effect as a whole and component-by-component and to suggest a comparatively simple quantity control method for the substance introduced into the target under SDP conditions. Numerical characteristics of these processes are determined using tungsten, iron, and alumina powders as the materials introduced into the target. A calculation method is proposed for determining the concentration of the material introduced into the target.

NOTATION

d , initial particle diameter; ρ , instantaneous density of the specimen; ρ_0 , initial density of the specimen; ρ_a , air density; ρ_w , density of distilled water; ρ_p , density of the powder particles; P_a and P_w , specimen mass in air and water, respectively; P_{th} , mass of the thread that supports the specimen; C , concentration of the introduced material in the target; q_{meas} , experimentally measured deviation of the specimen density from the initial value; q_{Fe50} , experimentally determined deviation of the specimen density from the initial value upon loading of the specimen with iron particles with $d < 50 \mu\text{m}$; q , absolute change in the specimen density due to introduction of

material with a density differing from the initial value; H and D , height (depth) and diameter of the target, respectively. Subscripts: a, air; w, water; th, thread.

REFERENCES

1. S. K. Andilevko, V. A. Shilkin, and S. M. Usherenko, *Int. J. Heat Mass Transfer*, **36**, No. 4, 1113-1124 (1993).
2. M. Jeandin, M. Vardavolias, S. K. Andilevko, O. V. Roman, V. A. Shilkin, and S. M. Usherenko, *Memoires et Etudes Scientifiques Revue de Metallurgie*, No. 12, 808-811 (1992).
3. S. K. Andilevko, O. V. Roman, V. A. Shilkin, and S. M. Usherenko, *Journal de Physique*, **IV**, 4, 795-801 (1994).
4. V. A. Vasil'eva, L. G. Voroshnin, V. G. Gorobtsov, and V. A. Shilkin, *Dokl. Akad. Nauk BSSR*, **32**, No. 2, 137-140 (1985).
5. S. M. Usherenko, V. F. Nozdrin, S. I. Gubenko, and G. S. Romanov, *Int. J. Heat Mass Transfer*, **37**, No. 15, 2367-2375 (1994).